HHS Public Access

Author manuscript

Arterioscler Thromb Vasc Biol. Author manuscript; available in PMC 2018 February 01.

Published in final edited form as:

Arterioscler Thromb Vasc Biol. 2017 February ; 37(2): 328–340. doi:10.1161/ATVBAHA.116.308507.

Rac2 Modulates Atherosclerotic Calcification by Regulating Macrophage IL-1β Production

Nicolle Ceneri[1,3,†], **Lina Zhao**[1,3,†], **Bryan D. Young**[3], **Abigail Healy**[1,2,3,4], **Suleyman Coskun**[3], **Hema Vasavada**[3], **Timur O. Yarovinsky**[3], **Kenneth Ike**[3], **Ruggero Pardi**[5], **Lingfen Qin**[1,3], **Li Qin**[3], **George Tellides**[1,3], **Karen Hirschi**[3], **Judith Meadows**[1,3], **Robert Soufer**[1,3], **Hyung J. Chun**[3], **Mehran M. Sadeghi**[1,3], **Jeffrey R. Bender**[3], and **Alan R. Morrison**[1,2,3,4,*]

[1]VA Connecticut Healthcare System, West Haven, Connecticut 06516, USA

[2]Providence VA Medical Center, Providence, Rhode Island 02908, USA

[3]Department of Internal Medicine (Section of Cardiovascular Medicine), Yale Cardiovascular Research Center, Yale University School of Medicine, New Haven, Connecticut 06511, USA

[4]Department of Internal Medicine (Section of Cardiovascular Medicine), Alpert Medical School at Brown University, Providence, Rhode Island, 02903 USA

[5]Department of Molecular Pathology, Universita Vita Salute School of Medicine, San Raffaele Scientific Institute, Milan, Italy

Abstract

Objective—The calcium composition of atherosclerotic plaque is thought to be associated with increased risk for cardiovascular events, but whether plaque calcium itself is predictive of worsening clinical outcomes remains highly controversial. Inflammation is likely a key mediator of vascular calcification, but immune signaling mechanisms that promote this process are minimally understood.

Approach and Results—Here we identify Rac2 as a major inflammatory regulator of signaling that directs plaque osteogenesis. In experimental atherogenesis, Rac2 prevented progressive calcification through its suppression of Rac1-dependent macrophage IL-1β expression, which in turn is a key driver of vascular smooth muscle cell calcium deposition by its ability to promote osteogenic transcriptional programs. Calcified coronary arteries from patients revealed decreased Rac2 expression but increased IL-1β expression, and high coronary calcium burden in patients with coronary artery disease was associated with significantly increased serum IL-1β levels. Moreover, we found that elevated IL-1β was an independent predictor of cardiovascular death in those subjects with high coronary calcium burden.

[*]To whom correspondence should be addressed: Alan R. Morrison, M.D., Ph. D., Providence VA Medical Center, Research (151), 830 Chalkstone Avenue, Providence, RI 02908, alan.morrison@yale.edu.

[†]These authors contributed equally to the study.

Author contributions: J.R.B. and A.R.M conceived the study. N.C., L.Z., B.D.Y., A.H., S.C., H.V., T.O.Y., K.I., R.P., K.H., H.J.C., M.S., J.R.B., and A.R.M. performed the *in vitro* and animal experiments. Lf.Q., G.T., L.Q., J.M., R.S., and A.R.M. performed the patient studies. N.C., L.Z., R.P., H.J.C., M.S., J.R.B., and A.R.M analyzed the data. N.C., L.Z., H.J.C., M.S., J.R.B., and A.R.M wrote the manuscript.

Disclosures: The authors have no disclosures to declare.

Conclusions—Overall, these studies identify a novel Rac2-mediated regulation of macrophage IL-1β expression, which has the potential to serve as a powerful biomarker as well as therapeutic target for atherosclerosis.

Introduction

Ischemic heart disease caused by atherosclerosis remains the single leading cause of morbidity and mortality in the world[1]. Traditional risk factor assessment, using gender, age, race, lipid profile, blood pressure, smoking, and diabetes is commonly used to risk stratify individuals with unestablished disease[2]. When applied to a diverse patient population, however, current risk assessment calculators can often overestimate risk in both men and women, resulting in substantial implications for the healthcare of individuals as well as to the cost of the healthcare system in general[3].

Coupling traditional risk assessment to a patient vulnerability bio-profile, using specific biomarkers, and structural information about plaque composition may enhance our ability to achieve improved risk stratification, moving cardiology toward an era of precision medicine[4–6]. One such example of plaque assessment is calcification, a widely studied pathologic finding that is thought to provide predictive values in terms of total atherosclerotic burden and risk of cardiovascular mortality and of all-cause mortality[7, 8]. Somewhat paradoxically, there has been a growing body of literature demonstrating that certain types of densely calcified plaques are associated with more stable disease[8–13]. In sum, these clinical studies highlight the potential value in defining mechanistic determinants of plaque calcium composition to better assess risk, but whether therapeutic modulation of the biologic processes that regulate plaque calcification might modify cardiovascular event risk will need to be determined.

Systemic inflammation as measured by high sensitivity C-reactive protein (hs-CRP), is an example of a well-established patient vulnerability factor that has predictive value in terms of cardiovascular events[14]. Although inflammation, in general, can be associated with formation of vascular calcification[15–19], the inflammatory mechanisms that can increase both atherosclerotic calcification and event risk are minimally understood. Moreover, there is significant controversy over whether inflammation and calcification work independently to promote increased event risk in patients or whether they are capable of working synergistically to promote increased risk[20–22].

Rac1 and Rac2 are key signal transducers in inflammatory cells, and Rac-based signaling influences the expression of a number of growth factors and cytokines[23–27]. Recently, we determined that *Rac2* deletion in macrophages led to reduced VEGF-A expression and consequent defects in inflammatory arteriogenesis in response to ischemia[26]. During our investigation, we identified that *Rac2* deletion also led to basal elevations in activated (GTP-bound) Rac1. Activated Rac1 can promote NF-κB signaling as well as reactive oxygen species production via NADPH oxidase; both known activators of the NLRP3 inflammasome protein complex that promotes IL-1β maturation[24, 28, 29]. We hypothesized that though the angiogenic macrophage responses were negatively affected by the *Rac2* deletion certain inflammatory macrophage responses may in fact be upregulated. Here, we

identify Rac2 as a critical determinant of the extent of macrophage Rac1-dependent IL-1β expression and consequent IL-1β-mediated atherosclerotic calcification. We demonstrate the robust efficacy of IL-1β inhibition in ameliorating experimental atherosclerosis. Most importantly, we identify a key correlation between elevated IL-1β serum levels and cardiovascular deaths in subjects with high vascular calcium burden. Overall, our findings highlight the importance of Rac2 mediated IL-1β suppression in regulation of vascular calcification and identify mechanistic basis for therapeutically targeting IL-1β in clinical atherosclerosis.

Materials and Methods

Materials and methods are available in the online-only Data Supplement.

Results

Calcified plaque is associated with increased IL-1β and decreased Rac2 expression

ApoE$^{-/-}$ mice were fed a high fat diet (HFD) to determine the relationship between Rac1 and Rac2 expression and plaque calcification. Near-infrared conjugated bisphosphonate compounds can bind to hydroxyapatite deposited by osteoblast-like cells during the mineralization of calcium, allowing for *ex vivo* molecular imaging and quantification of the calcification process[30, 31]. We found a modest increase in aortic calcification up to 14 weeks after start of HFD, but between 14 and 21 weeks there was a dramatic increase (Fig. 1 A , B). To begin investigating the role of Rac proteins in this context, Rac1 and Rac2 expression was assessed using RNA from the aortic arch. Initially, the hematopoietic-specific Rac2 expression rose in a manner corresponding to the influx of macrophages (as determined by F4/80), but at 21 weeks, Rac2 expression decreased despite sustained F4/80 expression (Fig 1C). These changes in the expression were limited to Rac2, as Rac1 expression was minimally altered over time. IL-1β expression trended toward a modest increase until 14 weeks, and between 14 and 21 weeks there was a significant increase that mirrored the rise in calcification.

To validate these findings in human atherosclerosis, we analyzed Rac expression using coronary samples from explanted human hearts of patients undergoing orthotopic heart transplant for ischemic cardiomyopathy. Left anterior descending coronary artery segments (1 cm) from the recently explanted human hearts were divided into two groups (calcified vs. noncalcified) based on the presence of calcium identified by noncontrast CT imaging using the Agatston method[32]; attenuation coefficient of >130 Hounsfield Units with an area of 3 or more pixels (Fig 1D). Neointimal plaque lesion area and calcification were confirmed by Elastic Van Gieson (EVG) staining of histological sections from the plaque (Fig 1E). We found comparable degrees of neointimal plaque burden in the two groups as assessed by measurement of the intima-to-media (I:M) thickness ratio (Fig. 1E,F), but the groups differed in terms of the presence or absence of plaque calcification. Interestingly, consistent with the calcified atherosclerosis of the mouse model, the relative Rac2 mRNA expression was significantly reduced in the human coronary segments containing calcified plaque whereas Rac1 expression and macrophage marker, CSF1R (CD115), expression remained constant (Fig. 1G–I). Of note, IL-1β expression was found to be significantly increased in

the coronary artery segments containing calcified plaque in a manner consistent with the animal model (Fig. 1J).

Rac2 deletion does not affect serum cholesterol or plaque lipid composition

To determine whether decreased Rac2 expression can promote vascular calcification, we evaluated the vascular phenotype of *Rac2* gene deletion on the $ApoE^{-/-}$ background. $Rac2^{+/+}ApoE^{+/+}$, $Rac2^{-/-}ApoE^{+/+}$, $Rac2^{+/+}ApoE^{-/-}$, and $Rac2^{-/-}ApoE^{-/-}$ mice developed normally, were of similar baseline weights, and had comparable weight increases on HFD (Supplemental Table I). $Rac2^{+/+}ApoE^{-/-}$ and $Rac2^{-/-}ApoE^{-/-}$ mice had comparable increases in total cholesterol and LDL in response to HFD (Supplemental Table II). Serum triglycerides were modestly elevated in the $Rac2^{-/-}ApoE^{-/-}$ mice. On the HFD, $Rac2^{+/+}ApoE^{-/-}$ and $Rac2^{-/-}ApoE^{-/-}$ mice demonstrated a similar peripheral blood monocytosis (Fig. IA). Gross atherosclerotic lipid burden of the aortas mirrored serum cholesterol levels with similar increases in Oil Red O positive areas in $Rac2^{+/+}ApoE^{-/-}$ and $Rac2^{-/-}ApoE^{-/-}$ mice relative to $Rac2^{+/+}ApoE^{+/+}$ and $Rac2^{-/-}ApoE^{+/+}$ mice (Fig. IB,C).

Hematoxylin and eosin staining of aortic sinus plaque and quantification of plaque area revealed similar plaque burden in $Rac2^{+/+}ApoE^{-/-}$ and $Rac2^{-/-}ApoE^{-/-}$ mice (Fig. ID,E). Quantification of the macrophage marker, F4/80, using RNA from the aortic arch, revealed no significant differences in expression in the $Rac2^{-/-}ApoE^{-/-}$ aortas relative to the $Rac2^{+/+}ApoE^{-/-}$ aortas (Fig. IF).

Rac2 deletion leads to increased plaque calcification

To define the role of Rac2 in vascular calcification, we analyzed plaque calcification by a combination of imaging and histology. Micro computed tomography (microCT) imaging demonstrated hypoattenuated lesions in the aortic sinuses and the lesser curvature of the aortic arches from $Rac2^{+/+}ApoE^{-/-}$ and $Rac2^{-/-}ApoE^{-/-}$ mice, corresponding to the established lipid plaque deposition (Fig. 2A, upper panels, black arrows). $Rac2^{-/-}ApoE^{-/-}$ aortas contained additional areas of hyperattenuation indicative of macrocalcification along the lesser curvature of the aortic arch (Fig. 2A, upper panels, yellow arrows), which was further confirmed by quantification of Alizarin Red staining (Fig. 2A, lower panels, and 2B). The global aortic calcification process was quantified using the targeted, near-infrared imaging probe (Fig. 2C,D). $Rac2^{-/-}ApoE^{-/-}$ aortas from mice on HFD for 14 weeks revealed significant increases in relative calcification over mice fed normal chow or control mice on a HFD. We further investigated the mechanistic basis of increased aortic calcification of the $Rac2^{-/-}ApoE^{-/-}$ mice. We found a significant enhancement of the osteogenic gene program in the atherosclerotic plaques of $Rac2^{-/-}ApoE^{-/-}$ mice relative to $Rac2^{+/+}ApoE^{-/-}$ mice, as demonstrated by significantly increased expression of the transcription factors, RUNX2, SOX9, OSX, and MSX2 (Fig. 2E). In addition, we found elevated expression (both RNA and protein) of the osteoblast maker alkaline phosphatase (ALP) in the $Rac2^{-/-}ApoE^{-/-}$ mice with a diffuse expression pattern as determined by immunofluorescent staining of the plaques (Fig 2E–G).

Increased vascular calcification of Rac2$^{-/-}$ mice is dependent on the hematopoietic compartment

To determine the cellular subpopulation involved in the increased calcification in *Rac2*$^{-/-}$*ApoE*$^{-/-}$ mice, we performed reciprocal bone marrow transplantation (Fig. 3A,B, II). Overall, aortic calcification burden was reduced in the autologous transplanted mice, consistent with prior reports that have demonstrated reduced thoracic aortic lesion area after irradiation and bone marrow transplant[33]. However, irradiated *Rac2*$^{-/-}$*ApoE*$^{-/-}$ mice subjected to autologous *Rac2*$^{-/-}$*ApoE*$^{-/-}$ transplantation maintained a significantly higher vascular calcification compared to *Rac2*$^{+/+}$*ApoE*$^{-/-}$ subjected to autologous *Rac2*$^{+/+}$*ApoE*$^{-/-}$ transplantation (Fig. 3A,B). Remarkably, transplantation of *Rac2*$^{-/-}$*ApoE*$^{-/-}$ bone marrow cells into *Rac2*$^{+/+}$*ApoE*$^{-/-}$ recipient mice led to significant increase in vascular calcification, whereas transplantation of *Rac2*$^{+/+}$*ApoE*$^{-/-}$ bone marrow cells into *Rac2*$^{-/-}$*ApoE*$^{-/-}$ recipient mice led to significantly decreased vascular calcification. Of note, IL-1β serum levels were significantly elevated in mice receiving the *Rac2*$^{-/-}$*ApoE*$^{-/-}$ bone marrow cells (Fig. 3C). In sum, both the increased calcification phenotype and protection from the phenotype were attributable to Rac2 function in the hematopoietic compartment, and calcification remained associated with elevated serum IL-1β.

Rac2 deletion leads to increased macrophage IL-1β expression

To identify specific signals regulated by Rac proteins that are critical to promoting the progressive calcification, cytokine mRNA profiling was performed on aortic arch tissues. Among multiple cytokines tested, IL-1β was the only factor that was significantly increased in the *Rac2*$^{-/-}$*ApoE*$^{-/-}$ aortas relative to the *Rac2*$^{+/+}$*ApoE*$^{-/-}$ aortas (Fig 3D). To assess whether the increase in IL-1β mRNA expression in calcified plaque reflected elevations in mature secreted IL-1β protein, we measured IL-1β protein from the serum. Systemic IL-1β concentrations were significantly higher in the *Rac2*$^{-/-}$*ApoE*$^{-/-}$ mice on HFD, whereas IL-1α and TNF-α concentrations did not differ significantly (Fig. 3E).

To further delineate the source of increased IL-1β, we conducted immunostaining of the atherosclerotic aortic plaques. IL-1β protein expression was elevated in the *Rac2*$^{-/-}$*ApoE*$^{-/-}$ aortic plaques and was predominantly restricted to macrophages as denoted by CD68 colocalization (Fig. 3F,G). To validate the role of Rac2 in negative regulation of macrophage IL-1β expression, we performed inflammasome stimulation of bone marrow derived macrophages (BMDMs) from *Rac*$^{+/+}$*ApoE*$^{-/-}$ and *Rac2*$^{-/-}$*ApoE*$^{-/-}$ mice using LPS priming and cholesterol crystal exposure. IL-1β production was significantly higher in *Rac2*$^{-/-}$*ApoE*$^{-/-}$ BMDM at each dose of cholesterol crystal tested (Fig. 4A). Moreover, IL-1β production was reduced toward baseline in *Rac2*$^{-/-}$*ApoE*$^{-/-}$ BMDMs reconstituted with either wild-type Rac2 or a constitutively active mutant of Rac2, Q61L (Fig. 4B,C), confirming Rac2 as a key determinant of macrophage IL-1β expression. In large part, Rac2 regulates IL-1β at the level of IL-1β mRNA expression (Fig. 4D).

There are several signaling pathways (*e.g.* NF-κB, NADPH-induced ROS) that may be upstream of inflammasome activation and IL-1β mRNA expression[34]. *Rac2*$^{-/-}$*ApoE*$^{-/-}$ BMDMs, transfected with an NF-κB responsive luciferase construct, demonstrated increased of NF-κB activation in response to LPS-primed cholesterol crystal exposure (Fig.

4E). In addition, *Rac2*$^{-/-}$*ApoE*$^{-/-}$ BMDMs revealed higher ROS production (Fig. 4F). To define the role of NF-κB and ROS production in the expression of IL-1β, BMDMs were stimulated to produce IL-1β in the presence or absence of an NF-κB inhibitor (celestrol), and an inhibitor of ROS production (diphenyleneiodium (DPI)). Both inhibitors decreased IL-1β protein secretion through reduced mRNA expression (Fig. 4G,H), while a p38-MAPK inhibitor, SB203580, had no effect on IL-1β expression (Fig. 4G,H, III). In sum, Rac2 deletion resulted in increased NF-κB activation and increased production of ROS, and macrophage IL-1β expression was dependent on these two signaling effectors.

Rac2 suppresses IL-1β expression via inhibition of Rac1 activity

Rac1 can promote activation of NF-κB as well as production of ROS via NADPH oxidase, both leading to inflammasome activation and IL-1β production[24, 28, 29]. To determine the influence of *Rac2* deletion on Rac1, we first explored the expression patterns of Rac1 and Rac2 in atherosclerotic plaque. Rac2 expression in atherosclerotic plaques from *Rac2*$^{+/+}$*ApoE*$^{-/-}$ mice was primarily limited to CD68+ cells relative to SMA+ cells (Fig. 5A,B). By contrast, Rac1 expression was comparable in CD68+ and SMA+ cells and remained constant in both the *Rac2*$^{+/+}$*ApoE*$^{-/-}$ and *Rac2*$^{-/-}$*ApoE*$^{-/-}$ plaques (Fig. 5C,D). We then explored the expression patterns of Rac1 and Rac2 in primary macrophages and primary mouse aortic smooth muscle cells (MASCMs) both at baseline and in response to inflammatory stimuli. Briefly, BMDMs and MASMCs from *Rac2*$^{+/+}$*ApoE*$^{-/-}$ *and* *Rac2*$^{-/-}$*ApoE*$^{-/-}$ mice underwent LPS-coupled cholesterol crystal exposure, and RNA was harvested to quantify relative Rac1 and Rac2 expression (Fig. IV). Rac2 expression could not be detected in *Rac2*$^{-/-}$*ApoE*$^{-/-}$ cells (negative control) or in any of the *Rac2*$^{+/+}$*ApoE*$^{-/-}$ MASMC conditions. In BMDMs, both Rac1 and Rac2 expression were upregulated as a consequence of LPS exposure, but Rac2 expression increased out of proportion to Rac1, supporting our *in vivo* findings in the aortic arch tissue that early inflammation influences the expression of Rac2. MASMCs revealed no change in Rac1 expression under any of the conditions consistent with their lack of IL-1β expression in plaque and overall lack of response to the LPS-coupled cholesterol exposure as a stimulus. There was no effect of *Rac2* deletion on Rac1 expression under any of the conditions in either the BMDMs or MASMCs. Despite relatively constant Rac1 expression, *Rac2*$^{-/-}$*ApoE*$^{-/-}$ BMDM lysates demonstrated significantly increased levels of GTP-Rac1 both at baseline and in a GTPγS dose-dependent manner (Fig. 5E,F). Taken in sum, Rac2 expression appeared limited to macrophages whereas Rac1 was expressed in both macrophages and smooth muscle cells, and *Rac2* deletion led to increased Rac1 activity despite having no effect on Rac1 expression.

To determine whether Rac1 activity was important in the elevated IL-1β expression associated with calcification in our model, we treated *Rac2*$^{-/-}$*ApoE*$^{-/-}$ BMDMs with an established Rac1 inhibitor (EHT 1864)[35], which led to a dose dependent decrease of IL-1β production (Fig. 5G). To exclude the possibility of destabilized cytoskeletal mobility by EHT 1864[35], we assessed whether this reduction in IL-1β production was due to reduced phagocytosis of cholesterol crystals. We found no significant difference in the phagocytosis of cholesterol crystals in *Rac2*$^{+/+}$*ApoE*$^{-/-}$ BMDMs and *Rac2*$^{-/-}$*ApoE*$^{-/-}$ BMDMs, with or without EHT 1864 treatment (Fig. V). To further validate our findings using a genetic model, we developed a myeloid genetic deletion of Rac1 (*CSF1R*^{mcm}*Rac1*$^{fl/fl}$). BMDMs

from *Rac2*$^{-/-}$*ApoE*$^{-/-}$*:CSF1R*^{mcm}*Rac1*$^{fl/fl}$ mice demonstrated complete loss of Rac1 expression in the setting of 4-hydroxytamoxifen (4-OHT) (Fig. 5F). Moreover, BMDMs from *Rac2*$^{-/-}$*ApoE*$^{-/-}$*:CSF1R*^{mcm}*Rac1*$^{fl/fl}$ mice demonstrated normalization of IL-1β protein expression, supporting the Rac1 dependence of increased IL-1β with Rac2 deletion. In sum, both Rac1 inhibition and *Rac1* deletion led to a loss in the enhanced IL-1β production conferred by the *Rac2* deletion.

Macrophage IL-1β targets vascular smooth muscle cells to promote vascular calcification

Inflammatory stimuli like LPS, TNF-α, or ROS can stimulate mesenchymal cells to mineralize calcium, but whether IL-1β plays a role in this process is somewhat controversial[15, 36, 37]. To assess whether *Rac2* gene deletion affects smooth muscle cell expression of IL-1β, we cultured primary mouse aortic smooth muscle cells (MASMCs) and performed inflammasome stimulation with LPS (10 ng/ml) followed by cholesterol crystal exposure (1000 μg/ml). BMDMs were used as a positive control for the expression of IL-1β. Using BMDMs as a control for the assay, MASMCs did not express detectable levels of IL-1β in response to LPS-coupled cholesterol crystal exposure nor were there any increases in IL-1β expression attributable to *Rac2* gene deletion (Fig. VI). To determine whether MASMCs might play a more responsive role to IL-1β, MASMCs from *ApoE*$^{-/-}$ mice were incubated with increasing concentrations of IL-1β and exhibited a dose-dependent response in terms of calcification (Fig. 6A,B). Moreover, consistent with our findings in the aortic plaques, MASMCs incubated in the presence or absence of IL-1β revealed increased expression of the osteogenic transcription factors, RUNX2, SOX9, OSX, and MSX2, as well as the osteoblast marker, ALP (Fig. 6C).

Calcification is dependent on IL-1β signaling

To determine whether the increased calcification found in *Rac2*$^{-/-}$*ApoE*$^{-/-}$ mice was, in fact, dependent on the increased expression of IL-1β, we inhibited IL-1 signaling using treatment with the IL-1 receptor antagonist (IL-1ra, anakinra) (Fig. VII). Treatment with IL-1ra prevented progression of calcification and revealed a modest trend toward calcific regression during the treatment period (Fig. 6D,E). Consistent with prior studies[38], treatment with IL-1ra reduced systemic IL-1β protein levels as measured by ELISA on serum samples (Fig. 6F). IL-1ra also prevented expansion of sinus plaque area (Fig. 6G,H). These findings confirm a cause-effect relationship between the increased IL-1β expression and the progressive atherosclerotic calcification.

Increased serum IL-1β level is a key predictor of cardiovascular endpoints in human coronary artery disease

To define the relationship between IL-1β protein levels and degree of atherosclerotic calcification, we identified a patient population with chronic stable coronary heart disease who underwent baseline blood draw for serum sample analysis and non-ECG-gated, non-contrast chest CT to allow for coronary artery calcium scoring (CACS). Serum IL-1β protein concentrations positively correlated with CACS (Fig. 7A). Patients were divided into two groups (low and high calcium burden) based on the CACS from the chest CT (Fig. 7B, Table I for patient demographics). There were no significant differences between the groups in terms of cardiac risk factors, including age, hypertension, hyperlipidemia, diabetes,

smoking, family history, and prior myocardial infarctions. There was a trend toward increased prior revascularization history in the high calcium burden group that did not meet statistical significance. Interestingly, we found a significantly higher median concentration of IL-1β in the high calcium burden group, supporting a strong clinical association between IL-1β levels and calcium burden (Table I and Fig. 7C).

To further elucidate the relevance of IL-1β levels and calcification regarding clinical outcomes, we assessed the frequency of cardiovascular events (sudden cardiac death, myocardial infarction, and acute coronary syndrome) between the two groups (Fig. 7D). There was a significantly increased hazard ratio in the high calcium burden group (4.88 (95% CI 1.03–22.98), $P = 0.045$). There was a total of 10 events; 6 sudden cardiac deaths, 1 ST segment elevation myocardial infarction (STEMI), 2 non-ST segment elevation myocardial infarctions (NSTEMIs), and 1 acute coronary syndrome (ACS). The differences between the two groups were primarily driven by sudden cardiac death. Next, we determined whether serum IL-1β level can serve as a further prognostic factor in these subjects. Both the low and high calcium burden groups were further subdivided into IL-1β ≤1.8 pg/ml and IL-1β >1.8 pg/ml groups based on the median IL-1β concentration in the low calcium burden group (Fig. 7E). We found that all of the cardiovascular events in both the low (n=2) and high (n=8) CACS groups occurred in subjects with elevated IL-1β levels, further implicating a key role for elevated IL-1β level as a prognostic indicator for worsening cardiovascular outcomes in individuals with established CAD.

Discussion

Calcification of atherosclerotic plaque is common in human disease, has been identified as a marker of disease burden, and is associated with risk of cardiovascular events[7, 8]. Recent data have demonstrated that the composition of calcium within individual plaques may predict vulnerability in some situations whereas stability in others, indicating there are likely additional factors that couple with calcification to alleviate or worsen risk[8–11, 39]. Inflammation is associated with calcification in animal models of disease, but there is ongoing debate as to whether inflammation can couple with calcification (*i.e.* “inflammatory calcification”) to promote increased cardiovascular event risk in patients[15–22]. We have identified a novel, inflammatory signaling axis that relies on Rac2 to modulate the level of Rac1-dependent macrophage IL-1β expression, which consequently determines extent of atherosclerotic calcification (See Fig. 8 Schematic).

The expression of Rac2 in macrophages was dynamic, rising with acute inflammation to dampen the immune response, as in the early atherogensis in the $ApoE^{-/-}$ model or in the early macrophage responses to LPS, but over time Rac2 expression returns toward a baseline, allowing for enhanced IL-1β expression in the setting of chronic inflammation. This enhanced IL-1β expression was modeled quite well by the *Rac2* deletion animals. The role of *Rac2* deletion in inflammatory, progressive atherosclerotic calcification was independent of lipid burden, as the atherosclerotic plaque lipid and the total serum cholesterol and LDL levels were unaffected. Comparable macrophage recruitment to atherosclerotic plaque indicated that Rac2 is essentially dispensable for macrophage migration and localization to plaque *in vivo*. However, *Rac2* deficiency did change the

calcium composition of the plaque, and moreover, Rac2 was found to be a major determinant for the degree of macrophage IL-1β expression. The differences in macrophage IL-1β expression conferred by *Rac2* gene deletion were directly dependent on Rac1, as demonstrated by studies using both pharmacologic or genetic abrogation of Rac1 signaling. The elevation of Rac1 activity in the setting of *Rac2* gene deletion is consistent with prior reports describing a compensatory relationship between Racs that results from complementary (albeit with some distinctions) roles in migration and activation of NADPH oxidase complex in myeloid cells[23, 40–42]. However, here we are able to define a novel, antagonistic relationship between Rac2 and Rac1 with regard to the signaling that regulates the expression of IL-1β. Further elucidation of the mechanisms behind this antagonistic relationship (*i.e.* competition for a common guanine nucleotide exchange factor) will be an important future direction of this work.

Both the bone marrow transplant data and the data confirming that $CD68^+$ cell populations express IL-1β in the plaques demonstrated a major role for the hematopoietic compartment, and more specifically macrophages, in our vascular calcification phenotype. In our study, MASMCs appeared to play an important responsive role to the IL-1β expressed by macrophages through the increased expression of osteogenic markers and enhanced calcium deposition. There is precedent for this responsiveness of vascular mesenchymal cells in a number of important early studies that have demonstrated *in vitro* calcifying vascular cells can express osteoblast-like markers such as alkaline phosphatase (ALP) in response to inflammatory stimuli, including lipopolysaccharide (LPS), tumor necrosis factor-α (TNF-α), or reactive oxygen species (ROS)[15, 36]. Moreover, there have been a number of outstanding studies of the vascular mesenchymal cell inflammatory response, which involves formation of matrix vesicles, plasma membrane-derived extra-cellular bodies and known to exhibit the proteins, matrix metalloproteinases, and phospholipids necessary for calcium mineralization, at the nidus of calcification[1615]. Recently, the protein, sortilin, has been shown to facilitate loading of the calcium mineralizing enzyme, alkaline phosphatase, into such extracellular vesicles to promote mesenchymal-driven calcification[43]. A close association between inflammatory macrophages and calcifying vascular cells appears required and in some studies involves either macrophage-secreted factors like TNF-α, or cell-cell contact through as yet unclear mechanisms to promote vascular calcification[15, 18, 19]. Previous studies have largely attributed activation of osteogenic gene programing largely to TNF-α, making the critical role of IL-1β in our model novel[19, 36, 44]. IL-1β has been established as important to early atherogenesis as an intermediary between lipid metabolism and activation of the immune system, but its role in calcific progression had remained somewhat controversial and unclear[37, 45]. Recently, a study of *IL-1ra* gene deletion demonstrated consequent increased aortic valve thickness that was associated with elevated TNF-α expression and that was abrogated by concomitant *TNF-α* gene deletion, supporting overlapping influence or possible interdependence of the two cytokines[46]. Yet in our study, TNF-α expression was not significantly altered as a result of the *Rac2* gene deletion. Given our finding of increased osteogenic transcription factor expression, including RUNX2, SOX9, OSX, and MSX2, from plaque tissue, our study raises the question of possible directs mechanism of IL-1 receptor signaling in the promotion of an osteogenic program in mesenchymal cells, and this will be an important future area of study.

Our *in vivo* studies using IL-1ra further demonstrate the causative role of IL-1β as a major determinant for the degree of plaque calcification. The retrospective analysis of our patient population with stable coronary disease reinforces the role of increased IL-1β in human vascular calcification. Most importantly, we provide pivotal clinical evidence that the combination of elevated IL-1β and high calcium burden was associated with worsened cardiovascular outcomes, indicating that elevated IL-1β levels in the setting of increased vascular calcification can serve as a critical determinant of plaque stability. Few clinical studies have measured IL-1β levels and successfully demonstrated a direct association with atherosclerotic burden much less atherosclerotic calcification or outcomes[47–49]. Though we acknowledge further study is required because our sample size is small and our study analysis is retrospective, no previous studies to date have demonstrated such a promising prognostic relevance for increased IL-1β levels with worsening outcomes in coronary artery disease[47, 49–51]. IL-1β inhibitory antibody (canakinumab) therapy is under evaluation for the reduction of secondary events in patients with ongoing inflammation after myocardial infarction[52]. Our mechanistic study outlines a critical signaling mechanism that provides fundamental understanding of the rationale for targeting this pathway as we attempt to bring treatment of cardiovascular patients into the era of precision medicine.

In summary, our findings demonstrate that the Rac2 expression is a key regulator of macrophage IL-1β expression and the consequent progressive calcification of atherosclerotic lesions. We anticipate this line of study will lead to development of novel, Rac-targeted therapeutic strategies that modulate plaque calcium composition to improve outcomes in individuals with coronary artery disease.

Supplementary Material

Refer to Web version on PubMed Central for supplementary material.

Acknowledgments

We thank Gaurav Choudhary for his outstanding and constructive feedback during the organization and preparation of the manuscript. We thank Swedish Orphan Biovitrum AB (SOBI) for their generous donation of anakinra for use in our studies.

Sources of Funding: This work was supported by Career Development Award Number 7IK2BX002527 from the United States Department of Veterans Affairs Biomedical Laboratory Research and Development Program (A.R.M.). The views expressed in this article are those of the authors and do not necessarily reflect the position or policy of the Department of Veterans Affairs or the United States government. This work was also supported in part by an Actelion ENTELLIGENCE Young Investigator Award (A.R.M.) and a CPVB COBRE Pilot Award NIH NIGMS P20GM103652. Additional funding support includes NIH grants F32 HL097422 (A.R.M.) and R01 HL043331 (J.R.B), a Raymond and Beverly Sackler Foundation Award (J.R.B.), and a Connecticut Biomedical Research Grant (J.R.B), and a CARPLO Foundation Award (R.P, J.R.B.). This work was also supported by NIH grant R01 HL113005 (H.C.), American Heart Association Established Investigator Award 14EIA17890000 (H.C.), and American Diabetes Association Basic Science Award 1-14-BS-035 (H.C.). This work was also supported by NIH grants UH3 EB017103, EB016629, and HL128064 (K.H.), as well as CT Innovations Grants 15-RMB-YALE-04 and 15-RMB-Yale-07 (K.H.).

Nonstandard Abbreviations and Acronyms

IL-1β	Interleukin-1 beta
LPS	Lipopolysaccharide

TNF-α	Tumor necrosis factor alpha
ROS	Reactive oxygen species
RUNX2	Runt-related transcription factor 2
MSX2	Msh homeobox 2
OSX	Osterix
SOX9	Sry-related HMG box 9
MAPK	Mitogen-activated protein kinase
NF-κB	Nuclear factor kappa-light-chain-enhancer of activated B cells
RhoGDI	Rho GDP-dissociation inhibitor
NADPH	Nicotinamide adenine dinucleotide phosphate
NLRP3	NACHT, LRR and PYD domains-containing protein 3
HFD	High fat diet (20%) supplemented by 1.25%, cholesterol
ELISA	Enzyme-linked immunosorbent assay
IL-1ra	Interleukin-1 receptor antagonist
MASMC	Mouse aorta smooth muscle cell
SMC	Smooth muscle cell
BMDM	Bone marrow derived macrophage

References

1. WHO. The 10 leading causes of death in the world, 2000 and 2012. 2012.
2. Goff DC Jr, Lloyd-Jones DM, Bennett G, et al. American College of Cardiology/American Heart Association Task Force on Practice G. 2013 acc/aha guideline on the assessment of cardiovascular risk: A report of the american college of cardiology/american heart association task force on practice guidelines. Circulation. 2014; 129:S49–S73. [PubMed: 24222018]
3. DeFilippis AP, Young R, Carrubba CJ, McEvoy JW, Budoff MJ, Blumenthal RS, Kronmal RA, McClelland RL, Nasir K, Blaha MJ. An analysis of calibration and discrimination among multiple cardiovascular risk scores in a modern multiethnic cohort. Annals of internal medicine. 2015; 162:266–275. [PubMed: 25686167]
4. Collins FS, Varmus H. A new initiative on precision medicine. The New England journal of medicine. 2015; 372:793–795. [PubMed: 25635347]
5. Naghavi M, Libby P, Falk E, et al. From vulnerable plaque to vulnerable patient: A call for new definitions and risk assessment strategies: Part ii. Circulation. 2003; 108:1772–1778. [PubMed: 14557340]
6. Naghavi M, Libby P, Falk E, et al. From vulnerable plaque to vulnerable patient: A call for new definitions and risk assessment strategies: Part i. Circulation. 2003; 108:1664–1672. [PubMed: 14530185]
7. Budoff MJ, Mao S, Zalace CP, Bakhsheshi H, Oudiz RJ. Comparison of spiral and electron beam tomography in the evaluation of coronary calcification in asymptomatic persons. International journal of cardiology. 2001; 77:181–188. [PubMed: 11182182]

8. Rennenberg RJ, Kessels AG, Schurgers LJ, van Engelshoven JM, de Leeuw PW, Kroon AA. Vascular calcifications as a marker of increased cardiovascular risk: A meta-analysis. Vascular health and risk management. 2009; 5:185–197. [PubMed: 19436645]
9. Criqui MH, Denenberg JO, Ix JH, McClelland RL, Wassel CL, Rifkin DE, Carr JJ, Budoff MJ, Allison MA. Calcium density of coronary artery plaque and risk of incident cardiovascular events. JAMA : the journal of the American Medical Association. 2014; 311:271–278. [PubMed: 24247483]
10. Motoyama S, Sarai M, Harigaya H, Anno H, Inoue K, Hara T, Naruse H, Ishii J, Hishida H, Wong ND, Virmani R, Kondo T, Ozaki Y, Narula J. Computed tomographic angiography characteristics of atherosclerotic plaques subsequently resulting in acute coronary syndrome. Journal of the American College of Cardiology. 2009; 54:49–57. [PubMed: 19555840]
11. Puchner SB, Liu T, Mayrhofer T, Truong QA, Lee H, Fleg JL, Nagurney JT, Udelson JE, Hoffmann U, Ferencik M. High-risk plaque detected on coronary ct angiography predicts acute coronary syndromes independent of significant stenosis in acute chest pain: Results from the romicat-ii trial. Journal of the American College of Cardiology. 2014; 64:684–692. [PubMed: 25125300]
12. Puri R, Nicholls SJ, Shao M, Kataoka Y, Uno K, Kapadia SR, Tuzcu EM, Nissen SE. Impact of statins on serial coronary calcification during atheroma progression and regression. Journal of the American College of Cardiology. 2015; 65:1273–1282. [PubMed: 25835438]
13. Irkle A, Vesey AT, Lewis DY, Skepper JN, Bird JL, Dweck MR, Joshi FR, Gallagher FA, Warburton EA, Bennett MR, Brindle KM, Newby DE, Rudd JH, Davenport AP. Identifying active vascular microcalcification by (18)f-sodium fluoride positron emission tomography. Nat Commun. 2015; 6:7495. [PubMed: 26151378]
14. Ridker PM. The jupiter trial: Results, controversies, and implications for prevention. Circulation. Cardiovascular quality and outcomes. 2009; 2:279–285. [PubMed: 20031849]
15. Aikawa E, Nahrendorf M, Figueiredo JL, Swirski FK, Shtatland T, Kohler RH, Jaffer FA, Aikawa M, Weissleder R. Osteogenesis associates with inflammation in early-stage atherosclerosis evaluated by molecular imaging in vivo. Circulation. 2007; 116:2841–2850. [PubMed: 18040026]
16. New SE, Goettsch C, Aikawa M, Marchini JF, Shibasaki M, Yabusaki K, Libby P, Shanahan CM, Croce K, Aikawa E. Macrophage-derived matrix vesicles: An alternative novel mechanism for microcalcification in atherosclerotic plaques. Circulation research. 2013; 113:72–77. [PubMed: 23616621]
17. Shanahan CM. Inflammation ushers in calcification: A cycle of damage and protection? Circulation. 2007; 116:2782–2785. [PubMed: 18071088]
18. Radcliff K, Tang TB, Lim J, Zhang Z, Abedin M, Demer LL, Tintut Y. Insulin-like growth factor-i regulates proliferation and osteoblastic differentiation of calcifying vascular cells via extracellular signal-regulated protein kinase and phosphatidylinositol 3-kinase pathways. Circulation research. 2005; 96:398–400. [PubMed: 15692088]
19. Tintut Y, Patel J, Territo M, Saini T, Parhami F, Demer LL. Monocyte/macrophage regulation of vascular calcification in vitro. Circulation. 2002; 105:650–655. [PubMed: 11827934]
20. Blaha MJ, Budoff MJ, DeFilippis AP, Blankstein R, Rivera JJ, Agatston A, O'Leary DH, Lima J, Blumenthal RS, Nasir K. Associations between c-reactive protein, coronary artery calcium, and cardiovascular events: Implications for the jupiter population from mesa, a population-based cohort study. Lancet. 2011; 378:684–692. [PubMed: 21856482]
21. Park R, Detrano R, Xiang M, Fu P, Ibrahim Y, LaBree L, Azen S. Combined use of computed tomography coronary calcium scores and c-reactive protein levels in predicting cardiovascular events in nondiabetic individuals. Circulation. 2002; 106:2073–2077. [PubMed: 12379576]
22. Reilly MP, Wolfe ML, Localio AR, Rader DJ. Study of Inherited Risk of Coronary A. C-reactive protein and coronary artery calcification: The study of inherited risk of coronary atherosclerosis (sirca). Arteriosclerosis, thrombosis, and vascular biology. 2003; 23:1851–1856.
23. Heasman SJ, Ridley AJ. Mammalian rho gtpases: New insights into their functions from in vivo studies. Nature reviews. Molecular cell biology. 2008; 9:690–701. [PubMed: 18719708]
24. Hordijk PL. Regulation of nadph oxidases: The role of rac proteins. Circulation research. 2006; 98:453–462. [PubMed: 16514078]

25. Li B, Yu H, Zheng W, Voll R, Na S, Roberts AW, Williams DA, Davis RJ, Ghosh S, Flavell RA. Role of the guanosine triphosphatase rac2 in t helper 1 cell differentiation. Science. 2000; 288:2219–2222. [PubMed: 10864872]
26. Morrison AR, Yarovinsky TO, Young BD, Moraes F, Ross TD, Ceneri N, Zhang J, Zhuang ZW, Sinusas AJ, Pardi R, Schwartz MA, Simons M, Bender JR. Chemokine-coupled beta2 integrin-induced macrophage rac2-myosin iia interaction regulates vegf-a mrna stability and arteriogenesis. The Journal of experimental medicine. 2014
27. Williams LM, Lali F, Willetts K, Balague C, Godessart N, Brennan F, Feldmann M, Foxwell BM. Rac mediates tnf-induced cytokine production via modulation of nf-kappab. Molecular immunology. 2008; 45:2446–2454. [PubMed: 18258304]
28. Arbibe L, Mira JP, Teusch N, Kline L, Guha M, Mackman N, Godowski PJ, Ulevitch RJ, Knaus UG. Toll-like receptor 2-mediated nf-kappa b activation requires a rac1-dependent pathway. Nature immunology. 2000; 1:533–540. [PubMed: 11101877]
29. Khan OM, Ibrahim MX, Jonsson IM, Karlsson C, Liu M, Sjogren AK, Olofsson FJ, Brisslert M, Andersson S, Ohlsson C, Hulten LM, Bokarewa M, Bergo MO. Geranylgeranyltransferase type i (ggtase-i) deficiency hyperactivates macrophages and induces erosive arthritis in mice. The Journal of clinical investigation. 2011; 121:628–639. [PubMed: 21266780]
30. Zaheer A, Lenkinski RE, Mahmood A, Jones AG, Cantley LC, Frangioni JV. In vivo near-infrared fluorescence imaging of osteoblastic activity. Nature biotechnology. 2001; 19:1148–1154.
31. Zaheer A, Murshed M, De Grand AM, Morgan TG, Karsenty G, Frangioni JV. Optical imaging of hydroxyapatite in the calcified vasculature of transgenic animals. Arteriosclerosis, thrombosis, and vascular biology. 2006; 26:1132–1136.
32. Agatston AS, Janowitz WR, Hildner FJ, Zusmer NR, Viamonte M Jr, Detrano R. Quantification of coronary artery calcium using ultrafast computed tomography. Journal of the American College of Cardiology. 1990; 15:827–832. [PubMed: 2407762]
33. Schiller NK, Kubo N, Boisvert WA, Curtiss LK. Effect of gamma-irradiation and bone marrow transplantation on atherosclerosis in ldl receptor-deficient mice. Arteriosclerosis, thrombosis, and vascular biology. 2001; 21:1674–1680.
34. Rathinam VA, Vanaja SK, Fitzgerald KA. Regulation of inflammasome signaling. Nature immunology. 2012; 13:333–342. [PubMed: 22430786]
35. Shutes A, Onesto C, Picard V, Leblond B, Schweighoffer F, Der CJ. Specificity and mechanism of action of eht 1864, a novel small molecule inhibitor of rac family small gtpases. The Journal of biological chemistry. 2007; 282:35666–35678. [PubMed: 17932039]
36. Sage AP, Tintut Y, Demer LL. Regulatory mechanisms in vascular calcification. Nature reviews. Cardiology. 2010; 7:528–536. [PubMed: 20664518]
37. Ikeda K, Souma Y, Akakabe Y, Kitamura Y, Matsuo K, Shimoda Y, Ueyama T, Matoba S, Yamada H, Okigaki M, Matsubara H. Macrophages play a unique role in the plaque calcification by enhancing the osteogenic signals exerted by vascular smooth muscle cells. Biochemical and biophysical research communications. 2012; 425:39–44. [PubMed: 22820183]
38. Goldbach-Mansky R, Dailey NJ, Canna SW, et al. Neonatal-onset multisystem inflammatory disease responsive to interleukin-1beta inhibition. The New England journal of medicine. 2006; 355:581–592. [PubMed: 16899778]
39. Joshi NV, Vesey AT, Williams MC, et al. 18f–fluoride positron emission tomography for identification of ruptured and high-risk coronary atherosclerotic plaques: A prospective clinical trial. Lancet. 2014; 383:705–713. [PubMed: 24224999]
40. Bokoch GM. Regulation of innate immunity by rho gtpases. Trends Cell Biol. 2005; 15:163–171. [PubMed: 15752980]
41. Yamauchi A, Kim C, Li S, Marchal CC, Towe J, Atkinson SJ, Dinauer MC. Rac2-deficient murine macrophages have selective defects in superoxide production and phagocytosis of opsonized particles. J Immunol. 2004; 173:5971–5979. [PubMed: 15528331]
42. Zhao X, Carnevale KA, Cathcart MK. Human monocytes use rac1, not rac2, in the nadph oxidase complex. The Journal of biological chemistry. 2003; 278:40788–40792. [PubMed: 12912997]

43. Goettsch C, Hutcheson JD, Aikawa M, et al. Sortilin mediates vascular calcification via its recruitment into extracellular vesicles. The Journal of clinical investigation. 2016; 126:1323–1336. [PubMed: 26950419]
44. Al-Aly Z, Shao JS, Lai CF, Huang E, Cai J, Behrmann A, Cheng SL, Towler DA. Aortic msx2-wnt calcification cascade is regulated by tnf-alpha-dependent signals in diabetic ldlr−/− mice. Arteriosclerosis, thrombosis, and vascular biology. 2007; 27:2589–2596.
45. Duewell P, Kono H, Rayner KJ, et al. Nlrp3 inflammasomes are required for atherogenesis and activated by cholesterol crystals. Nature. 2010; 464:1357–1361. [PubMed: 20428172]
46. Isoda K, Matsuki T, Kondo H, Iwakura Y, Ohsuzu F. Deficiency of interleukin-1 receptor antagonist induces aortic valve disease in balb/c mice. Arteriosclerosis, thrombosis, and vascular biology. 2010; 30:708–715.
47. Correia LC, Andrade BB, Borges VM, Clarencio J, Bittencourt AP, Freitas R, Souza AC, Almeida MC, Leal J, Esteves JP, Barral-Netto M. Prognostic value of cytokines and chemokines in addition to the grace score in non-st-elevation acute coronary syndromes. Clin Chim Acta. 2010; 411:540–545. [PubMed: 20083097]
48. Ikonomidis I, Andreotti F, Economou E, Stefanadis C, Toutouzas P, Nihoyannopoulos P. Increased proinflammatory cytokines in patients with chronic stable angina and their reduction by aspirin. Circulation. 1999; 100:793–798. [PubMed: 10458713]
49. Kilic T, Ural D, Ural E, Yumuk Z, Agacdiken A, Sahin T, Kahraman G, Kozdag G, Vural A, Komsuoglu B. Relation between proinflammatory to anti-inflammatory cytokine ratios and long-term prognosis in patients with non-st elevation acute coronary syndrome. Heart. 2006; 92:1041–1046. [PubMed: 16547209]
50. Orn S, Ueland T, Manhenke C, Sandanger O, Godang K, Yndestad A, Mollnes TE, Dickstein K, Aukrust P. Increased interleukin-1beta levels are associated with left ventricular hypertrophy and remodelling following acute st segment elevation myocardial infarction treated by primary percutaneous coronary intervention. Journal of internal medicine. 2012; 272:267–276. [PubMed: 22243053]
51. Van Tassell BW, Toldo S, Mezzaroma E, Abbate A. Targeting interleukin-1 in heart disease. Circulation. 2013; 128:1910–1923. [PubMed: 24146121]
52. Ridker PM, Thuren T, Zalewski A, Libby P. Interleukin-1beta inhibition and the prevention of recurrent cardiovascular events: Rationale and design of the canakinumab anti-inflammatory thrombosis outcomes study (cantos). American heart journal. 2011; 162:597–605. [PubMed: 21982649]

Highlights

- Rac2 is a major negative regulator of atherosclerotic plaque IL-1β expression through inhibition of macrophage Rac1-dependent IL-1β production.
- Atherosclerotic calcification is dependent on IL-1β and inhibition of IL-1β signaling effectively ameliorates experimental atherosclerosis.
- Elevated serum IL-1β is associated with cardiovascular death in patients with high coronary calcium burden.

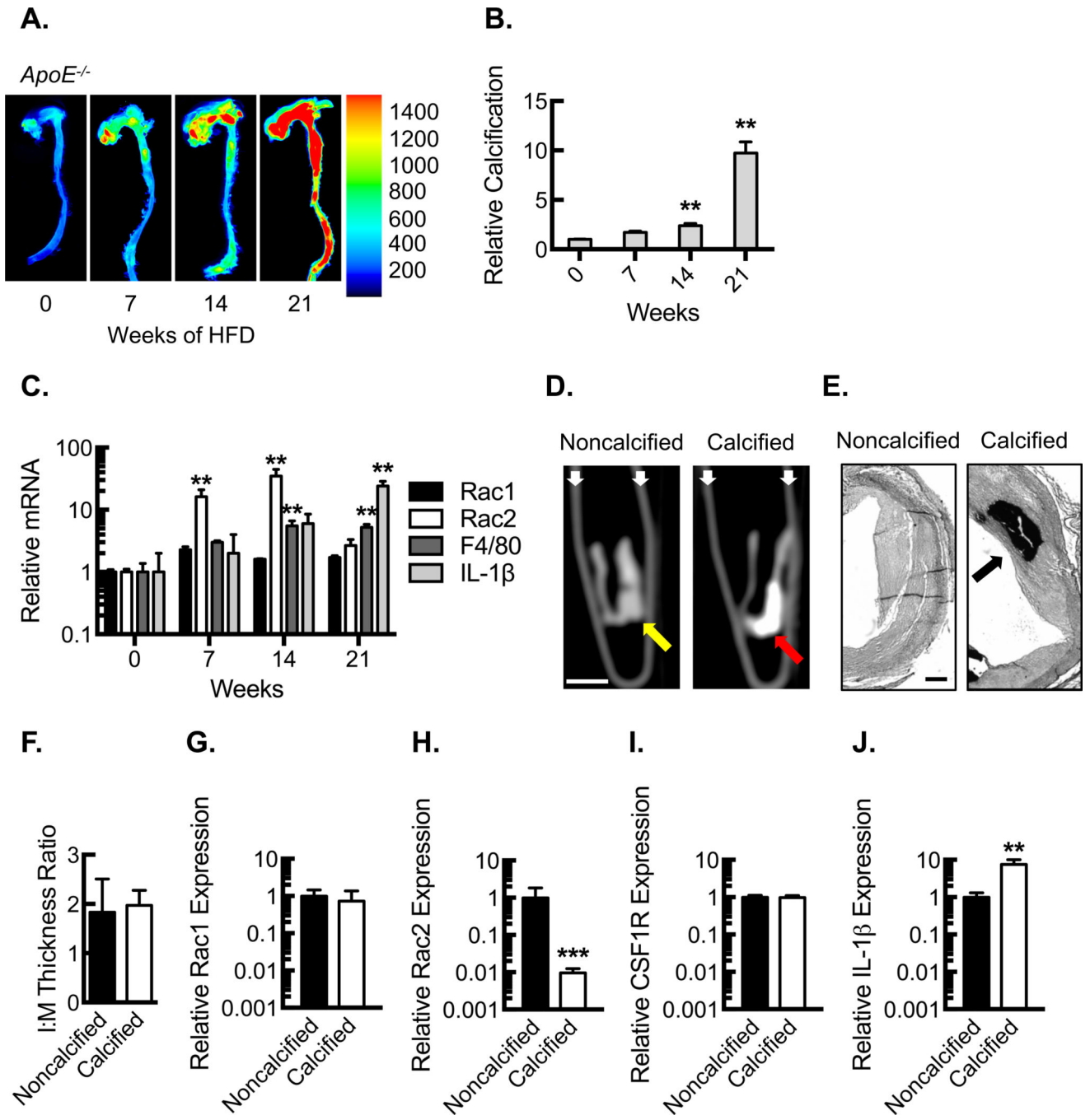

Figure 1. Calcified plaque is associated with increased IL-1β and decreased Rac2 expression

(A) *Ex vivo* near-infrared calcium imaging from *ApoE*$^{-/-}$ mice fed a HFD over 21 weeks along with quantification (B) of relative calcification signal (**, P<0.05; n=5 animals per time point). (C) Quantification (relative to time 0) of mRNA expression for Rac1, Rac2, F4/80, and IL-1β in aortic arches from *ApoE*$^{-/-}$ mice fed a HFD over 21 weeks (**, P<0.05, n=5 animals per time point). (D) CT micrographs of 1 cm human proximal LAD segments in longitudinal axis illustrating calcified plaque as identified by the Agatston method. White bar, 0.5 cm. White small arrows, microcentrifuge tube wall. Yellow arrow, atherosclerotic

wall segment without calcification. Red arrow, atherosclerotic wall segment with calcification. (E) Elastic Van Gieson staining of human left coronary artery sections (proximal to segments in D) from explanted hearts along with morphometric analysis (F), quantifying intima:media (I:M) thickness ratio (n=5 individual subjects). Black bar, 500 μm. Black arrow, calcification. Real-time PCR quantification of Rac1 (G), Rac2 (H), CSF1R (I) and IL-1β (J) mRNA expression from noncalcified vs. calcified human LAD coronary segments from D (***, P<0.001; **, P<0.05; n=5 individual subjects). All data are representative of at least 3 independent experiments. Quantitative data are displayed as mean ± SEM.

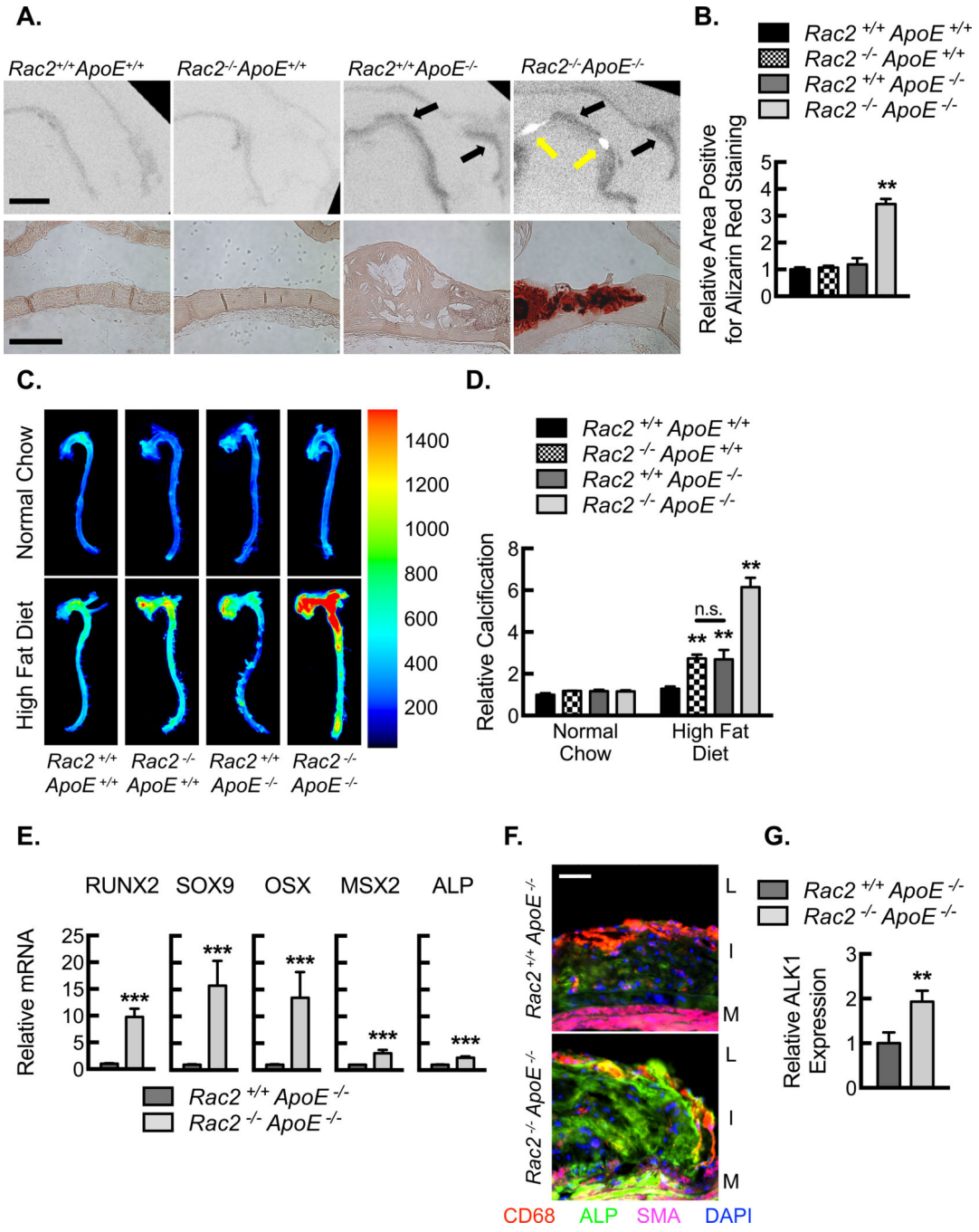

Figure 2. *Rac2* deletion results in increased plaque calcification

(A) *Ex vivo* MicroCT images (Upper Panels; Bar, 1000 μm) of aortic arches from mice fed HFD for 14 weeks along with micrographs (Lower Panels; Bar, 250 μm) of lesser arch tissue sections stained for Alizarin red. Black arrows indicate the dark luminal irregularities of lipid accumulation. Yellow arrows denote white areas of calcification. (B) Quantification of percent wall area positive for Alizarin Red Staining from aortic arches in A (**, P<0.05; *n*=8 animals). (C) *Ex vivo* near-infrared calcium imaging from mice on normal chow or HFD for 14 weeks along with quantification (D) of relative calcification signal (**, P<0.05; *n*=8

animals). (E) Real-time PCR quantification of mRNA isolated from aortic arch tissue after mice were fed a HFD for 14 weeks for the transcription factors, RUNX2, SOX9, OSX, and MSX2, as well as ALP (**, P<0.05; *n*=8 animals). (F) Immunofluorescence micrographs of aortic plaques from *Rac2*$^{+/+}$*ApoE*$^{-/-}$ and *Rac2*$^{-/-}$*ApoE*$^{-/-}$ mice demonstrating expression of ALP (green), CD68 (red), and SMA (magenta). Nuclei counterstained with DAPI (blue). Bar, 50 μm. Lumen, L. Intimal lesion, I. Media, M. (G) Quantification of relative ALP expression in aortic plaques from F (**, P<0.05; *n*=8 animals). All data are representative of at least 3 independent experiments. Quantitative data are displayed as mean ± SEM.

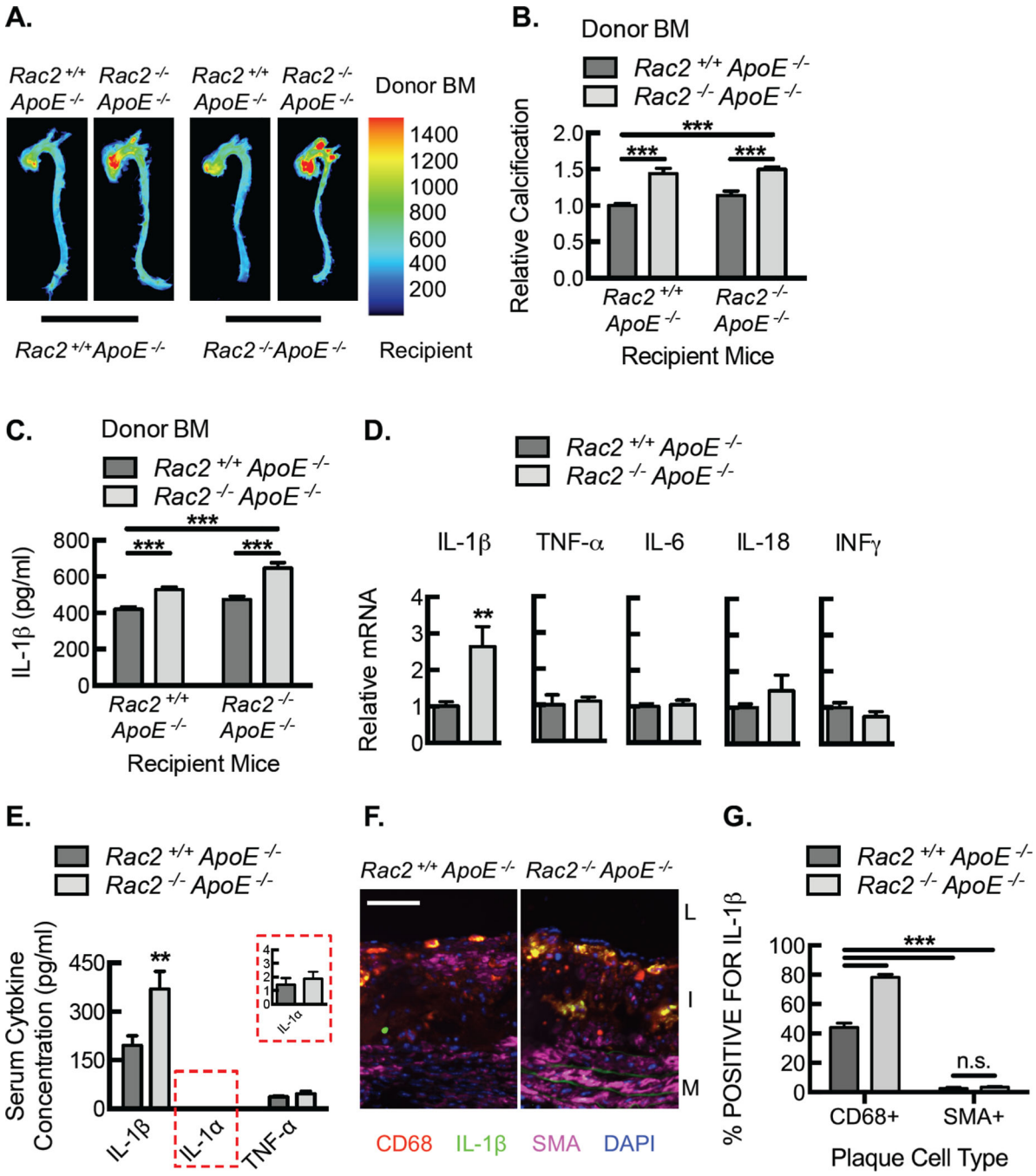

Figure 3. Vascular calcification in *Rac2*$^{-/-}$ mice depends on the hematopoietic compartment and is associated with increased macrophage IL-1β expression

(A) *Ex vivo* near-infrared calcium imaging of aortas along quantification of relative calcification (B) signal and serum IL-1β levels (C) from reciprocal bone marrow transplants, using *Rac2*$^{+/+}$*ApoE*$^{-/-}$ and *Rac2*$^{-/-}$*ApoE*$^{-/-}$ mice (**, P<0.05 n=6 animals). (D) Real-time PCR quantification of mRNA isolated from aortic arch plaque tissue after mice were fed a HFD for 14 weeks for the following cytokines: IL-1β, TNF-α, INFγ, IL-18, and IL-6 (**, P<0.05; n=8 animals). (E) Serum IL-1β, IL-1α, and TNF-α protein concentrations by ELISA from *Rac2*$^{+/+}$*ApoE*$^{-/-}$ and *Rac2*$^{-/-}$*ApoE*$^{-/-}$ and mice after HFD for 14 weeks (**,

P<0.05; *n*=8 animals with each data point being an average of two technical replicates). (F) Immunofluorescence micrographs of aortic plaques from *Rac2*$^{+/+}$*ApoE*$^{-/-}$ and *Rac2*$^{-/-}$*ApoE*$^{-/-}$ mice demonstrating expression of IL-1β (green), CD68 (red), and SMA (magenta). Nuclei counterstained with DAPI (blue). Bar, 170 μm. Lumen, L. Intimal lesion, I. Media, M. (G) Quantification of percent cells positive for IL-1β in aortic plaques from F (**, P<0.05; *n*=8 animals). All data are representative of at least 3 independent experiments. Quantitative data are displayed as mean ± SEM.

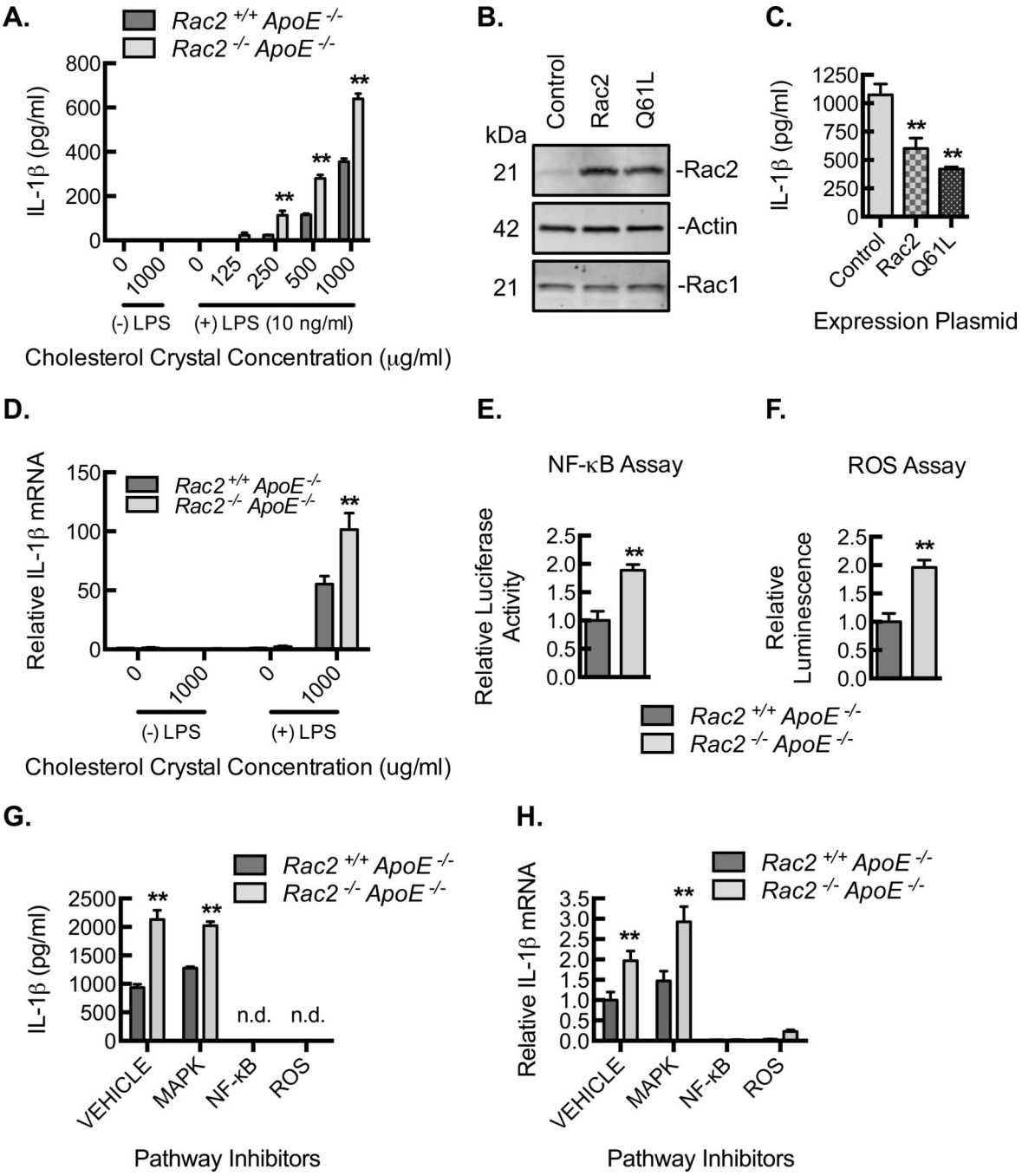

Figure 4. *Rac2*$^{-/-}$ deletion is associated with increased NF-κB- and ROS-dependent IL-1β expression

(A) Resting or LPS-primed BMDMs from *Rac2*$^{+/+}$*ApoE*$^{-/-}$ and *Rac2*$^{-/-}$*ApoE*$^{-/-}$ mice were treated with cholesterol crystals at indicated concentrations for 24 hours, and ELISA for IL-1β was performed on culture supernatants (**, P<0.05; n=3 animals with each animal data point being an average of 3 technical repeats). (B) Representative Rac2, actin, and Rac1 immunoblots of BMDM lysates from *Rac2*$^{-/-}$*ApoE*$^{-/-}$ mice after BMDMS were transfected with GFP alone (control) or GFP with wild-type Rac2 (Rac2) or with constitutively active Rac2 (Q61L). (C) BMDMs, transfected as in (B), were primed with LPS and treated with

1000 μg/mL cholesterol crystals for 24 hours, and ELISA for IL-1β was performed on culture supernatants (**, P<0.05; *n*=3 animals with each animal data point being an average of 3 technical repeats). (D) Real-time PCR quantification of IL-1β mRNA isolated from resting or LPS-primed BMDMs that were treated with 1000 μg/mL cholesterol crystals for 24 hours (**, P<0.05; *n*=3 animals with each animal data point being an average of 3 technical repeats). (E) Relative luciferase activity in $Rac2^{+/+}ApoE^{-/-}$ and $Rac2^{-/-}ApoE^{-/-}$ BMDMs transfected with a NF-κB responsive luciferase construct and then stimulated by LPS-primed cholesterol crystal exposure (**, P<0.05; 3 animals with each animal data point being an average of 3 technical repeats). (F) Relative luminescence as a measure of ROS production in $Rac2^{+/+}ApoE^{-/-}$ and $Rac2^{-/-}ApoE^{-/-}$ BMDMs stimulated by LPS-primed cholesterol crystal exposure (**, P<0.05; *n*=3 animals with each animal data point being an average of 3 technical repeats). (G) $Rac2^{+/+}ApoE^{-/-}$ and $Rac2^{-/-}ApoE^{-/-}$ BMDMs were pretreated with DMSO (vehicle control), SB203580 (MAPK inhibitor, 10 μM), celastrol (NF-κB inhibitor, 5 μM) or Diphenyleneiodonium (DPI; reactive oxygen species inhibitor, 10 μM) and then LPS-primed and treated with cholesterol crystals for 3 hours, and ELISA for IL-1β was performed on culture supernatants (** P<0.05; *n*=6 mice per group). (H) Real-time PCR quantification of mRNA isolated from BMDMs in G for IL-1β (**, P<0.05 $Rac2^{-/-}ApoE^{-/-}$ relative to $Rac2^{+/+}ApoE^{-/-}$; *n*=6 mice per group). All data are representative of at least 3 independent experiments. Quantitative data are displayed as mean ± SEM.

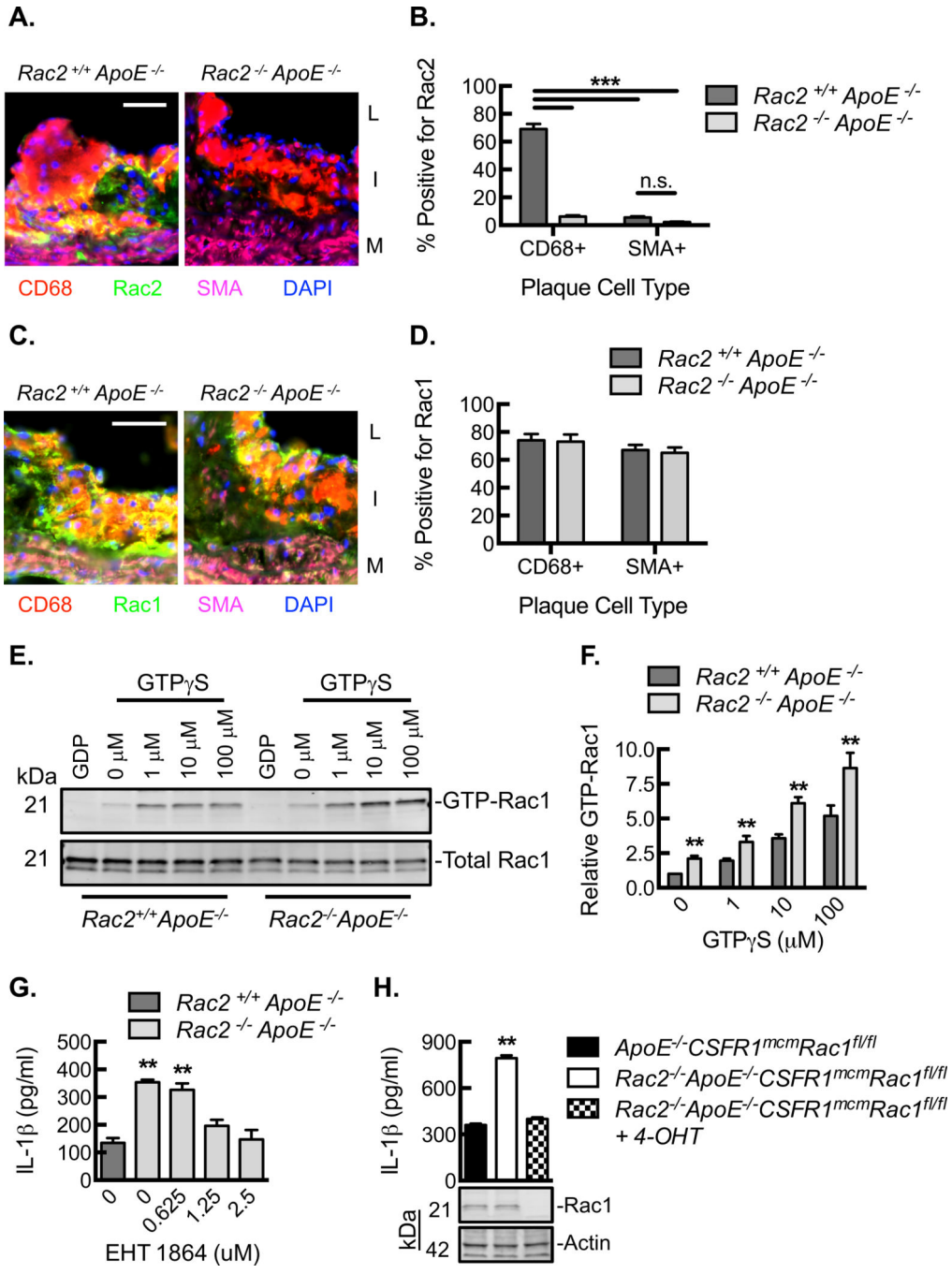

Figure 5. Macrophage Rac2 regulates Rac1-dependent IL-1β expression

(A) Immunofluorescence micrographs of aortic plaques from *Rac2*$^{+/+}$*ApoE*$^{-/-}$ and *Rac2*$^{-/-}$*ApoE*$^{-/-}$ mice demonstrating expression of Rac2 (green), CD68 (red), and SMA (magenta). Nuclei counterstained with DAPI (blue). Bar, 50 μm. Lumen, L. Intimal lesion, I. Media, M. (B) Quantification of percent cells positive for Rac2 in aortic plaques from A (***, P<0.001; *n*=8 animals). (C) Immunofluorescence micrographs of aortic plaques from *Rac2*$^{+/+}$*ApoE*$^{-/-}$ and *Rac2*$^{-/-}$*ApoE*$^{-/-}$ mice demonstrating expression of Rac1 (green), CD68 (red), and SMA (magenta). Nuclei counterstained with DAPI (blue). Bar, 50 μm.

Lumen, L. Intimal lesion, I. Media, M. (D) Quantification of percent cells positive for Rac1 in aortic plaques from C (n=8 animals). (E) Rac1 immunoblot of BMDM lysates from $Rac2^{+/+}ApoE^{-/-}$ and $Rac2^{-/-}ApoE^{-/-}$ mice loaded with increasing GTPγS concentrations for 5 minutes at 37°C, after which GTP-Rac1 was affinity precipitated by PBD pulldown along with quantification of GTP-bound Rac1 (F) (**, P<0.05; n=3 animals with each animal data point being an average of 3 technical repeats). (G) LPS-primed BMDMs from $Rac2^{+/+}ApoE^{-/-}$ and $Rac2^{-/-}ApoE^{-/-}$ mice were treated with 1000 μg/ml cholesterol crystals in the absence or presence of Rac1 inhibitor, EHT 1864, at indicated concentrations (**, P<0.05; n=3 animals with each animal data point being an average of 3 technical repeats). (H) LPS-primed BMDMs from $ApoE^{-/-}CSF1R^{mcm}Rac1^{fl/fl}$ and $Rac2^{-/-}ApoE^{-/-}CSF1R^{mcm}Rac1^{fl/fl}$ mice pre-treated with or without 4-hydroxytamoxifen (4-OHT) were exposed to 1000 μg/mL cholesterol crystals for 24 hours, and ELISA for IL-1β was performed on culture supernatants (**, P<0.05; n=3 animals with each animal data point being an average of 3 technical repeats). Lower panel, Rac1 and actin immunoblots of BMDM lysates. All data are representative of at least 3 independent experiments. Quantitative data are displayed as mean ± SEM.

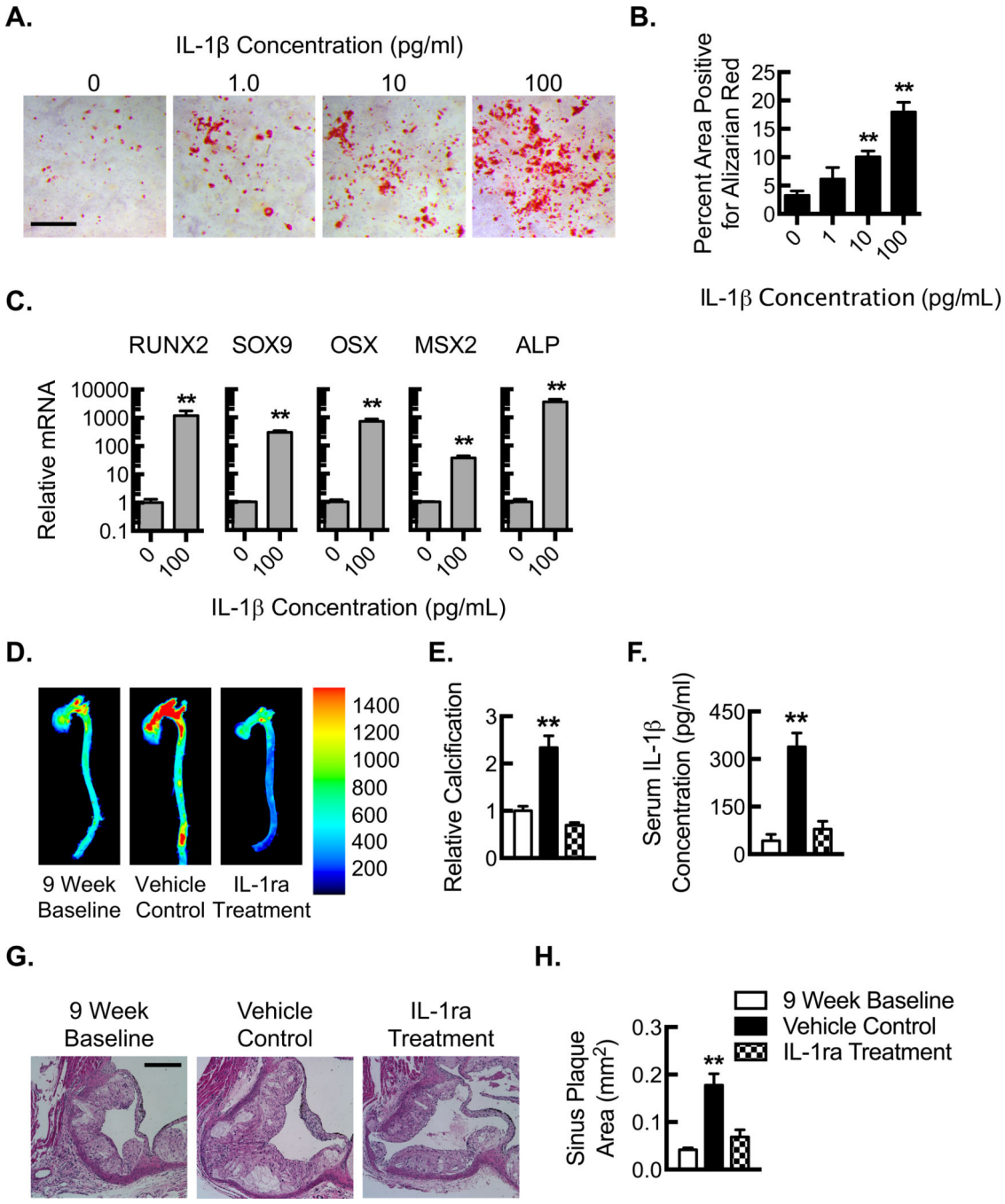

Figure 6. IL-1β stimulates vascular smooth muscle cells calcification and atherosclerotic calcification is dependent on IL-1β signaling

(A) Photomicrographs along with quantification (B) of Alizarin red staining for mineralized calcium from cultured primary mouse aortic smooth muscle cells (*ApoE*$^{-/-}$) that were treated with increasing concentrations of IL-1β for 21 days (**, P<0.05; *n*=6 animals with each animal data point being an average of 3 technical repeats). Scale bar 1000 μm. (C) Real-time PCR quantification of RUNX2, SOX9, OSX, MSX2, and ALP in mRNA samples isolated from primary mouse aortic smooth muscle cells (*ApoE*$^{-/-}$) that were treated with 0 or 100 pg/mL of recombinant IL-1β for 21 days (**, P<0.05; *n*=6 animals with each animal

data point being an average of 3 technical repeats). (D) Near-infrared calcium imaging along with quantification (E) of calcification signal in *ex vivo* aortas from *Rac2*$^{-/-}$*ApoE*$^{-/-}$ mice after HFD for 9 weeks to establish baseline and then after an additional 5 weeks of HFD coupled to treatment with vehicle control or IL-1ra (**, P<0.05 *n*=8 animals). (F) Serum IL-1β protein concentrations by ELISA (**, P<0.05; *n*=8 animals). (G) Hematoxylin and eosin staining of adjacent aortic sinus sections at the level of the aortic valve after HFD for 9 weeks to establish baseline and then after an additional 5 weeks of HFD coupled to treatment with vehicle control or IL-1ra. Bar, 200 μm. (H) Quantification of average aortic plaque area (**, P<0.05; *n*=9 aortic valve sinuses from 3 animals). All data are representative of at least 3 independent experiments. Quantitative data are displayed as mean ± SEM.

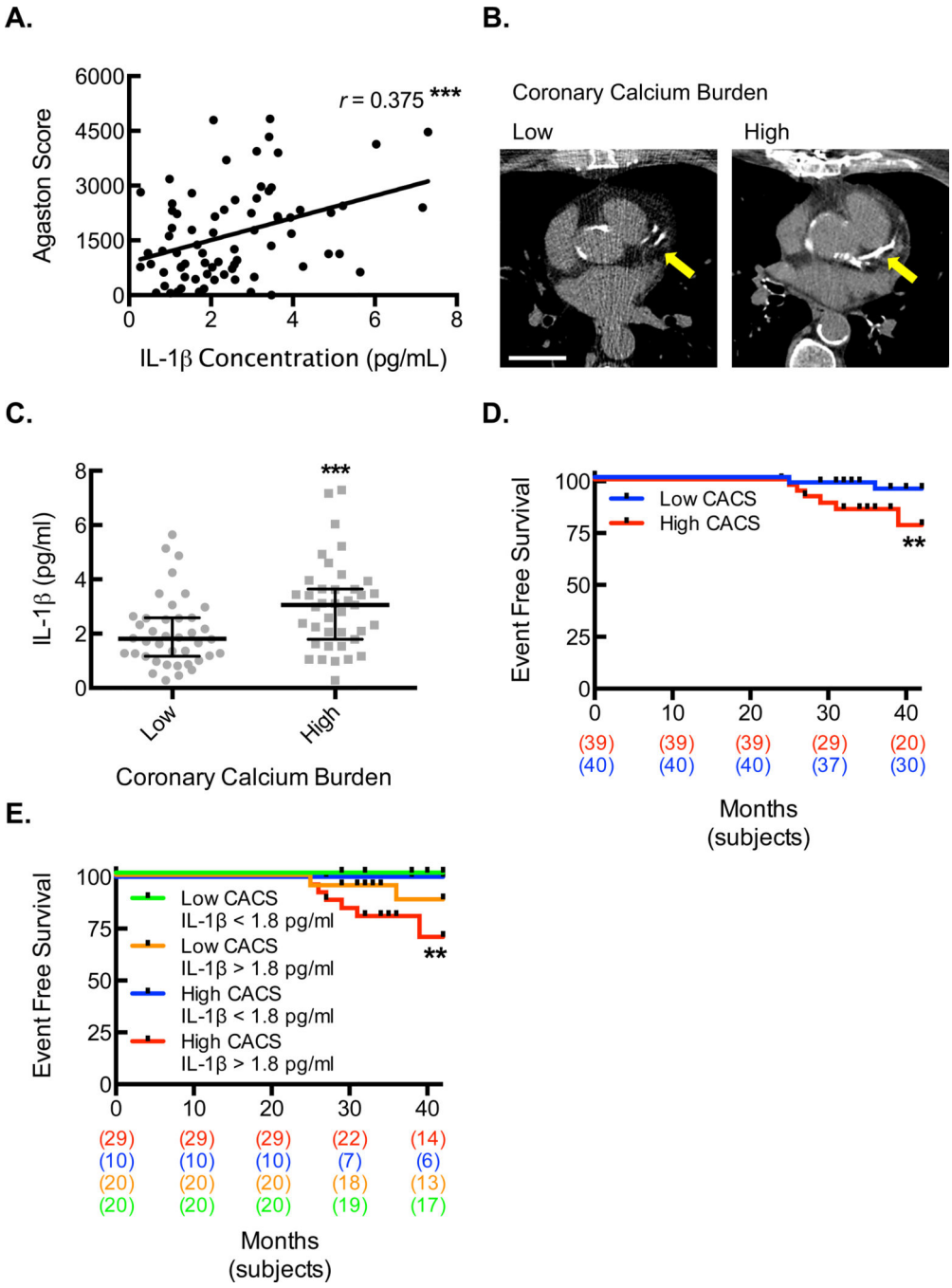

Figure 7. Increased serum IL-1β level is associated with higher coronary calcium burden and is predictive of cardiovascular outcomes in patients

(A) The Pearson correlation between IL-1β protein concentrations and CACS (***, P=0.001; *n*=79). (B) Noncontrast CT scan images illustrating the LAD territory calcification in coronary disease patients who were divided by CACS into low and high calcium burden groups. Bar, 3 cm. (C) Serum IL-1β protein concentrations for each patient (gray dots) along with median and interquartile ranges within each level of calcium burden (***, P=0.0040; *n*=39–40). (D) Kaplan-Meier event curve for hard cardiac events of sudden cardiac death, myocardial infarction, and acute coronary syndrome in patients divided by calcium burden

(**, P=0.0259, n=39–40, long-rank test). (E) Kaplan-Meier event curve for hard cardiac events of sudden cardiac death, myocardial infarction, and acute coronary syndrome in patients divided by both calcium burden and serum IL-1β concentration (**, P=0.0119, n=10–28, long-rank test).

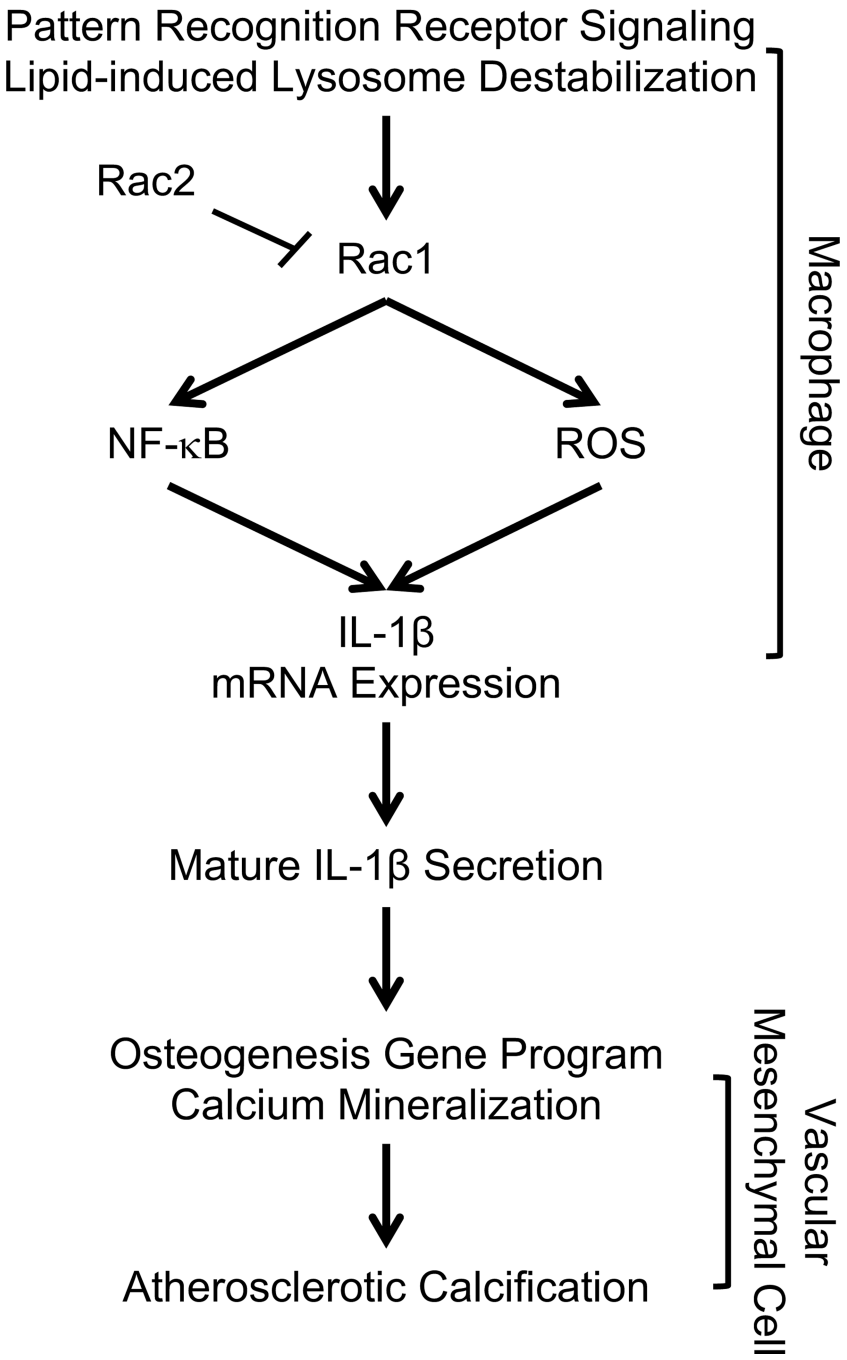

Figure 8. Summary Schematic

Pattern recognition receptor signaling (*i.e.* Toll-like receptor signaling) coupled to cholesterol crystal induced lysosomal destabilization by phagocytic cells like macrophages promotes Rac-modulated expression of IL-1β. Rac2 is a major determinant of the degree of macrophage IL-1β expression by regulating Rac1 activity upstream of NF-κB, and ROS. Macrophage Rac2 and Rac1 exist in a state of balance with Rac2 serving as a brake that tempers Rac1-dependent IL-1β expression. When the Rac2 brake is released, as in the chronic inflammation associated with atherosclerosis or as modeled in the *Rac2*$^{-/-}$*ApoE*$^{-/-}$

mouse, IL-1β expression is enhanced, resulting in the upregulation of mesenchymal cell osteogenic transcription factors and the consequent mineralization of calcium.

TABLE I

Baseline Demographics and Clinical Characteristics by Calcium Burden

	Low (*n*=40)	**High (*n*=39)**	**P Value**
Age, years, mean ± SEM	64.3 ± 1.3	68.1 ± 1.5	0.062
Male, *n* (%)	38 (95.0)	38 (97.4)	1.00
DM, *n* (%)	12 (30.0)	18 (46.2)	0.14
Hypertension, *n* (%)	39 (97.5)	37 (94.9)	0.62
Hyperlipidemia, *n* (%)	40 (100)	39 (100)	NA
Family History of Early CAD, *n* (%)	9 (23.1)	7 (17.9)	0.57
Smoking History, *n* (%)	29 (74.4)	29 (74.4)	1.00
MI, *n* (%)	19 (47.5)	18 (46.2)	0.90
Prior Revascularization (PCI or CABG), *n* (%)	29 (72.5)	35 (89.7)	0.051
Time from baseline serum to CT, months, median (IQR)	9 (4, 26)	16 (5, 26)	0.56
CACS, median (IQR)	758.3 (421.6, 1043.7)	2650.4 (2228.4, 4134.7)	<0.0001****
IL-1β, pg/mL, median (IQR)	1.81 (1.17, 2.58)	3.06 (1.79, 3.64)	0.0040***